Implicit large eddy simulations with a high-order TENO scheme

Lin Fu *, Xiangyu Y. Hu and Nikolaus A. Adams

Institute of Aerodynamics and Fluid Mechanics, Technische Universität München, 85748 Garching, Germany
*Correspondent author: lin.fu@tum.de

ABSTRACT

Although TENO schemes, proposed by Fu *et al.* (2016), show promising results for turbulence reproduction, they are unsuitable to function as a reliable subgrid LES model by generating excessive dissipation. Meanwhile, the state-of-the-art implicit LES models, e.g. the localized artificial diffusivity scheme by Kawai *et al.* (2010), typically depend on shock sensors, which are case-dependent and fail to retain the monotonicity near discontinuities. The difficulty locates on scale-separating the low-wavenumber smooth regions, high-wavenumber fluctuations and discontinuities sufficiently and incorporating adequate dissipation into numerical schemes correspondingly. In this paper, we propose a new 8-point 6th-order TENO8-A scheme, which is motivated for gas dynamics and physics-consistent for incompressible and compressible turbulence modeling. While the low-wavenumber smooth region is handled by the optimized linear scheme, with the measurement of local flow scales, the high-wavenumber fluctuations and discontinuities are predicted with adaptive nonlinear dissipation. The new scheme is Galilean invariant and free from physics-based sensors rendering its high generality. Benchmark simulations demonstrate that, while the TENO8-A scheme exhibits exceptional performance in gas dynamics, it faithfully reproduces the kinetic energy evolution for incompressible turbulence and predicts the vorticity, entropy and acoustic modes as good as the physics-motivated ILES models for compressible turbulence decay.

Introduction

Large Eddy Simulation (LES) is an attractive research topic as it can faithfully reproduce the large-scale flow structures with much less computational efforts compared to Direct Numerical Simulation (DNS). Explicit LES method employs a physics-motivated subgrid scale (SGS) model and makes great achievements. However, the performance strongly depends on a tailored low-dissipation high-order scheme as the interaction between the numerical truncation error and the SGS model introduces extra uncertainties. On the other hand, the implicit LES (ILES) method, where the discretization truncation error of convective terms functions as a subgrid-scale model, attracts increasing attentions in recent years. The previous attempts in ILES simulations, e.g. the flux-corrected transport (FCT) method, the piecewise parabolic (PPM) method and weighted essentially non-oscillatory (WENO) method, show promising results.

Recently, a family of high-order targeted ENO (TENO) schemes has been proposed by Fu *et al.* (2016). Main properties of TENO schemes are: (i) arbitrarily high-order odd (upwind) or even (central) schemes can be constructed within a unified framework; (ii) the order-degeneration problem is avoided and the spectral properties of a nonlinear TENO scheme recover to that of its corresponding linear scheme for low to intermediate wavenumbers; (iii) spectral optimization results in order reduction by one.

Main Objectives

In this work, based on the recently proposed shock-capturing targeted ENO (TENO) Fu *et al.* (2016) concept, we propose a new 6th-order 8-point TENO8-A scheme, which

1. shows good performances for gas dynamics;
2. is physics-consistent for incompressible and compressible turbulence reproduction, i.e. reliable as an ILES model;
3. without parameter tuning case by case;
4. satisfies the Galilean invariant property and without physical-variable based sensors;
5. without spurious numerical oscillations and overshoots for highly-compressible gas dynamics simulations;
6. is able to recover the Kolmogorov scaling for infinite Reynolds number under-resolved simulations of incompressible flows;
7. is capable of predicting the vorticity, entropy and acoustic models faithfully for compressible turbulence;
8. without numerical difficulties for typical benchmark simulations.

Numerical Methods

1. Within certain stencil points, the counterpart linear scheme features high-order accuracy while maintaining the minimum dispersion and the approximate dispersion relation. The full stencil width should be large enough to model the turbulence spatial correlation.
2. In order to tolerate turbulence, extreme low nonlinear dissipation is produced for the high-wavenumber physical fluctuations. On the other hand, enough nonlinear dissipation is generated for the sharp discontinuity capturing.
3. The low-wavenumber flow scales are isolated and handled by pure optimal linear scheme without compromise. Here, the low-wavenumber region is defined to range from wavenumber 0 to approximate 1;

Results

In this section, a set of benchmark cases motivated for the gas dynamics, incompressible and compressible turbulence is simulated. At the cell interface, the ROE method is applied for the characteristic decomposition. The Rusanov scheme by Rusanov (1961) is employed for the flux computing by default while in some specific cases ROE-type scheme is simulated for comparisons. The 3rd-order TVD Runge-kutta method Gottlieb *et al.* (2001) is adopted for the time integral of governing equations. The CFL number is set as 0.4 if not mentioned otherwise. For all simulations, TENO8-A employs the recommended parameters without tuning to demonstrate the case-independent property.

0.1 Double Mach reflection of a strong shock

The initial condition is Woodward (1984)

$$(\rho,u,v,p)=\begin{cases}(1.4,0,0,1), & \text{if } y<1.732(x-0.1667),\\ (8,7.145,-4.125,116.8333), & \text{otherwise .}\end{cases} \tag{1}$$

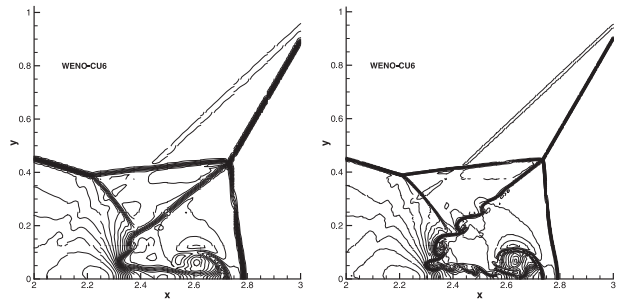

Figure 1. Double Mach reflection of a strong shock: density contours from the WENO-CU6 scheme at simulation time $t = 0.2$. Resolution of 512×128 (left) and 1024×256 (right). This figure is drawn with 43 density contours between 1.887 and 20.9.

The computational domain is $[0,4] \times [0,1]$ and the simulation end time is $t = 0.2$. Initially, a right-moving Mach 10 shock wave is placed at $x = 0.1667$ with an incident angle of 60^0 to the x-axis. The post-shock condition is imposed from $x = 0$ to $x = 0.1667$ whereas a reflecting wall condition is enforced from $x = 0.1667$ to $x = 4$ at the bottom. For the top boundary condition, the fluid variables are defined to exactly describe the evolution of the Mach 10 shock wave. The inflow and outflow condition are imposed for the left and right sides of the computational domain.

For comparison, the results from the WENO-CU6 scheme at resolution of 512×128 and 1024×256 are given in Fig. 1.

We run this case with mesh resolution of 400×100, 512×128 and 800×200. As shown in Fig. 2, even with lower resolutions, TENO8-A performs much better than WENO-CU6 in resolving the small-scale fluctuations in the "blown-up" portion while the shock-wave structures, e.g. the Mach stems, are captured sharply without distinguished oscillations. Note that the present TENO8-A scheme does not suffer from numerical difficulty for the high-resolution simulations while the classical low-dissipation WENO-CU6-M scheme fails (see Fig.18 of Fu *et al.* (2016)). In particular, except that from the other TENO family schemes (see Fig.18 of Fu *et al.* (2016)), no comparable results from the WENO schemes of similar stencil points at a similar resolution, can be figured out in the literatures (see Fig.1 of Shi *et al.* (2003), Fig.10 of Castro *et al.* (2011), and Fig.20 of Gerolymos *et al.* (2009)).

0.2 Incompressible Taylor-Green vortex

The initial condition with well-resolved single-mode velocity field is set as Brachet *et al.* (1983*b*)

$$\begin{aligned} &u(x,y,z,0) = \sin(x)\cos(y)\cos(z), \\ &v(x,y,z,0) = -\cos(x)\sin(y)\cos(z), \\ &w(x,y,z,0) = 0, \\ &\rho(x,y,z,0) = 1.0, \\ &p(x,y,z,0) = 100 + \tfrac{1}{16}[(\cos(2x)+\cos(2y))(2+\cos(2z)) - 2], \end{aligned} \tag{2}$$

and the nearly incompressible property is reproduced for the entire simulation. The computational domain is $[0,2\pi] \times [0,2\pi] \times [0,2\pi]$ with periodic boundary condition enforced at six sides.

0.2.1 Viscous simulation

For viscous simulations, a good scheme or turbulent model should not affect the instability modes of the laminar flow and faithfully reproduce the laminar-turbulent transition. The classical Smagorinsky model is demonstrated to fail in this case without further modification Hickel *et al.* (2006)Lesieur (2012). For a under-resolved simulation, a coarse

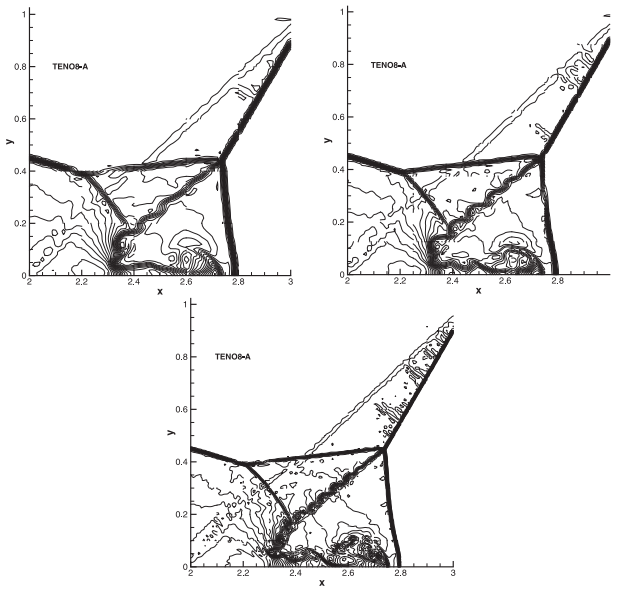

Figure 2. Double Mach reflection of a strong shock: density contours from the TENO8-A scheme at the simulation time $t = 0.2$. Resolution of 400×100 (top left), 512×128 (top right) and 800×200 (bottom). This figure is drawn with 43 density contours between 1.887 and 20.9.

mesh consisting of 64^3 uniform grid points is employed. To assess the numerical dissipation and physical consistence of proposed scheme, the Reynolds numbers ranging from $Re = 100$ to $Re = 3000$ are considered. The numerical results from the state-of-the-art implicit LES model ALDM Hickel *et al.* (2006) on the same resolution and from the DNS of Brachet *et al.* (1983*a*) on a mesh of 256^3 are provided for comparisons. The simulations with the conventional Smagorinsky model and the dynamic Smagorinsky model at the same resolution can be found in Hickel *et al.* (2006) and not duplicated here.

As shown in Fig. 3, at the low Reynolds number 100 and 200, the ALDM model is slightly more dissipative than TENO8-A for laminar flow reproducing. For the Reynolds number 400, it is noted that TENO8-A performs much better in the later time stage from $t = 8$ to $t = 10$. With increasing Reynolds number, both ALDM and TENO8-A show good agreement with the DNS reference and predict the peak of dissipation rate in the later time stage very well. For the pure laminar flow before $t = 4$, the ALDM model exhibits excessive numerical dissipation while the result from TENO8-A almost exactly matches the DNS data. The proper explanation is that the TENO8-A scheme is 6th-order accurate which enables it recover the exact spectra in the low-wavenumber region while the 2nd-order ALDM model loses the accuracy in these regions. Moreover, although the classical WENO-CU6-M scheme is particularly optimized for the inviscid case towards recovering the Kolmogorov scaling in all resolved wavenumbers, the performance in these finite Reynolds number simulations is not comparable to present result (see Fig. 7 and Fig. 8 of Schranner *et al.* (2013)). It is also noted that the numerical results from the latest version of ALDM and the new developed ILES method (see Fig. 6 in Egerer *et al.* (2016)) are far from present result either.

0.3 Compressible isotropic turbulence decay

The three-dimensional decaying compressible isotropic turbulence with shocklets is studied. For high turbulent Mach number

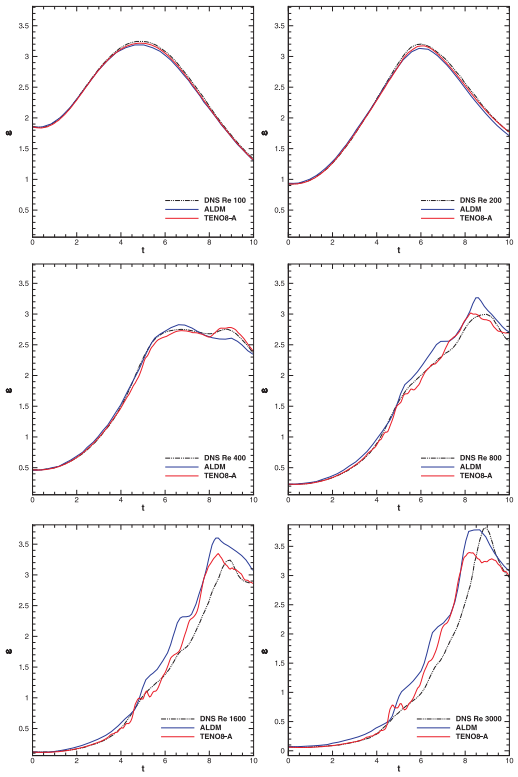

Figure 3. Incompressible viscous Taylor-Green vortex: comparisons of energy dissipation rate on a 64^3 mesh. The dark dashed line denotes the DNS reference produced on a 256^3 mesh Brachet *et al.* (1983*a*); the red solid line denotes the result from the TENO8-A scheme while the blue line denotes that from the ALDM model (digitized from Hickel *et al.* (2006)).

$M_{t_0} = \frac{\sqrt{3}u_{rms,0}}{\langle c \rangle} = 0.6$ with $u_{rms} = \sqrt{\langle u_i u_i \rangle / 3}$, weak shocklets develop spontaneously from the turbulent motion and therefore it greatly challenges the resolving capability of proposed numerical scheme for broadband flow in the presence of shock waves Johnsen *et al.* (2010)Kawai *et al.* (2010)Kotov *et al.* (2016)Arshed & Hoffmann (2013). This case has been widely investigated with the DNS simulation, explicit/implicit LES models and high-order shock-capturing methods.The three-dimensional Navier-Stokes equations are solved in the computational domain $[0,2\pi]\times[0,2\pi]\times[0,2\pi]$ with periodic boundary conditions. The initial Reynolds number is set as $\mathrm{Re}_{\lambda_0} = \frac{\langle\rho\rangle u_{rms,0}\lambda_0}{\langle\mu\rangle} = 100$, where the Taylor-scale is defined $\lambda = \frac{1}{3}\sum_i \sqrt{\frac{\langle u_i^2\rangle}{\left\langle \left(\frac{\partial u_i}{\partial x_i}\right)^2 \right\rangle}} = 0.5$. The initial condition consists of a random solenoidal velocity field satisfying the power spectra given by

$$E(k) \sim k^4 \exp(-2(k/k_0)^2),\ \frac{\langle u_{i,0}u_{i,0}\rangle}{2} = \frac{3u_{rms,0}^2}{2} = \int_0^\infty E(k)dk, \tag{3}$$

where k_0 determines the wavenumber where the spectrum peaks and is set as $k_0 = 4$ in the current simulation. The other parameters are defined as

$$\rho_0 = u_{rms,0} = T_0 = 1, \gamma = 1.4, \mathrm{Pr} = 0.7. \tag{4}$$

The viscosity is assumed to obey the power law as $\frac{\mu}{\mu_{ref}} = (\frac{T}{T_{ref}})^{0.75}$ and the eddy turn over time $\tau = \frac{\lambda_0}{u_{rms,0}}$ is adopted as the time scale.

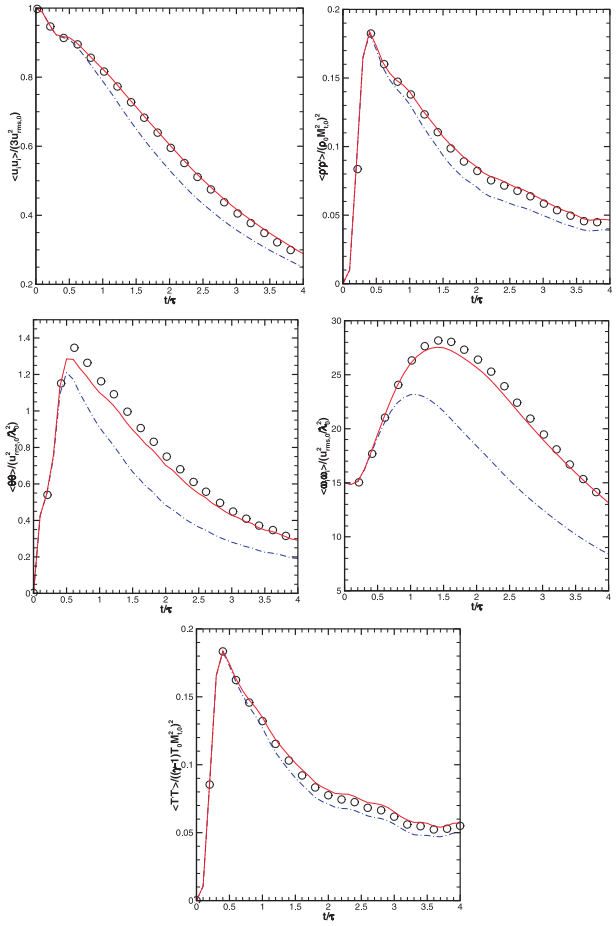

Figure 4. Compressible isotropic turbulence decay: comparisons of temporal evolutions of variance of different quantities on a 64^3 mesh. Circles denote the filtered DNS reference from that produced on a 256^3 mesh Johnsen *et al.* (2010); the red solid line denotes the result from the TENO8-A scheme while the blue dashed line denotes that from the WENO-CU6 scheme.

The simulation is run until the end time $t/\tau = 4$. In the above definition, the bracket $\langle\cdot\rangle$ denotes the statistic average over the computational domain. The heat transfer and the viscous effect are computed with a 4th-order central scheme.

Fig. 4 gives the histories of computed normalized mean-square velocity, density fluctuation, dilatation, enstrophy and temperature fluctuation. While WENO-CU6 under-estimates all the measured statistics suggesting its excessive built-in dissipation, the results from TENO8-A agree with the filtered DNS reference very well. When compared with that from the state-of-the-art localized artificial diffusivity scheme LAD-D2-0 (see Fig.4 in Kawai *et al.* (2010)), the TENO8-A scheme performs slightly better in predicting the mean-square velocity and density fluctuation, significantly better in reproducing the dilatation while slightly under-estimating the enstrophy. Meanwhile, the performance of TENO8-A is as good as that of the C10-AV12 scheme (see Fig.7 in Kotov *et al.* (2016)).

Fig. 5 gives the spectra of the velocity, density, dilatation and vorticity computed by the WENO-CU6 and TENO8-A scheme. It is noted that WENO-CU6 is very dissipative for all the physical modes and the result agrees with the reference solution for a very small range of resolved wavenumbers. On the contrary, TENO8-A shows good agreement with the DNS for a large range of wavenumbers. Particularly, the computed density spectra matches with the DNS data up to the Nyquist wavenumber. Compared with the LAD-

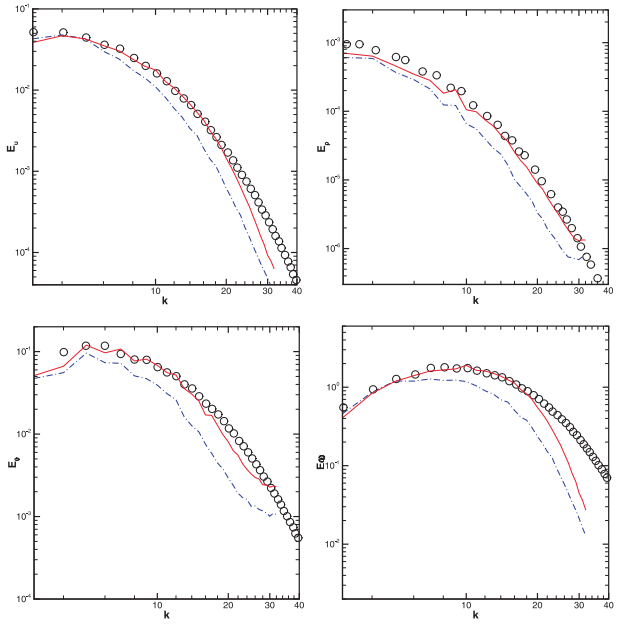

Figure 5. Compressible isotropic turbulence decay: comparisons of spectrum at the end simulation time $\frac{t}{\tau} = 4$ on a 64^3 mesh. Circles denote the DNS reference on the 256^3 mesh Johnsen *et al.* (2010); the red solid line denotes the result from the TENO8-A scheme while the blue dashed line denotes that from the WENO-CU6 scheme.

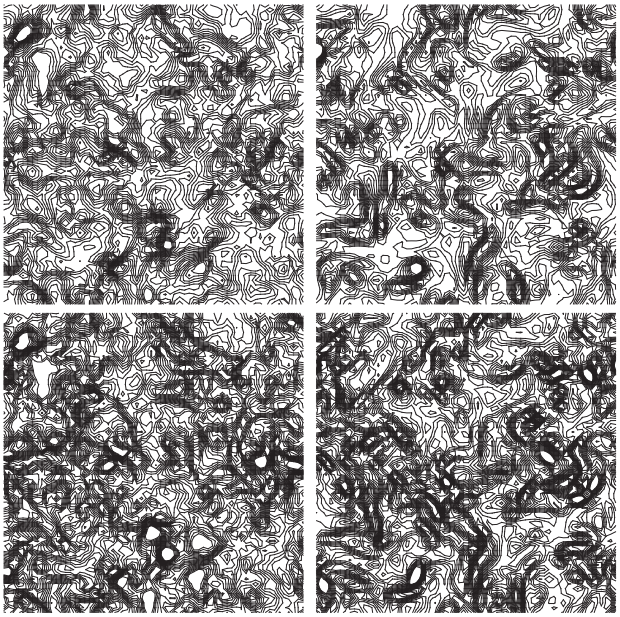

Figure 6. Compressible isotropic turbulence decay: comparisons of computed dilatation (left) and x-component vorticity (right) contours from the WENO-CU6 scheme (top) and the TENO8-A scheme (bottom) in the middle section of x-axis at the nondimensional time $\frac{t}{\tau} = 4$. 20 equally spaced contours are drawn from -1 to 1 for the dilatation while from -5 to 5 for the x-component vorticity. The mesh resolution is $64 \times 64 \times 64$.

D2-0 scheme (see Fig.6 in Kawai *et al.* (2010)), TENO8-A performs much better in the prediction of dilatation mode while other computed spectra are comparable. Moreover, the unphysical energy pile-up at high wavenumbers, which occurs to all the presented schemes in paper Kotov *et al.* (2016) (see Fig. 8), is not observed in present result.

As shown in Fig. 6, compared with WENO-CU6, the TENO8-A scheme resolves much stronger dilatation and much richer vorticities, implying its low-dissipation property. The classical WENO schemes, including the well-optimized scheme with parameter tuning for this case (see Fig. 10 and Fig. 11 of Arshed & Hoffmann (2013), Fig. 11 and Fig. 13 of Johnsen *et al.* (2010)), are far from playing the role of subgrid model for compressible turbulence.

In order to demonstrate the convergence and robustness of the proposed TENO8-A scheme, we study this case at a higher resolution of $128 \times 128 \times 128$. As shown in Fig. 7, with the increased resolution, the computed kinetic energy and vorticity spectrum converge to the DNS results on a 256^3 mesh. Fig. 8 shows the resolved vortical structures on both resolutions.

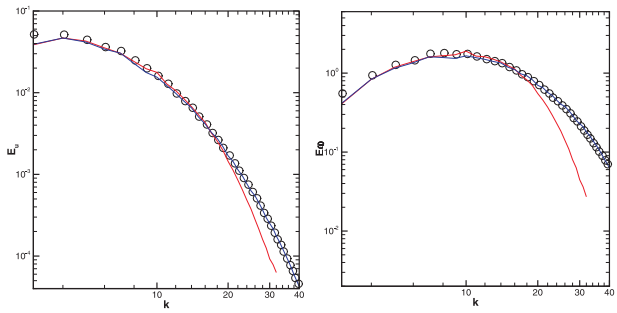

Figure 7. Compressible isotropic turbulence decay: comparisons of spectrum at the end simulation time $\frac{t}{\tau} = 4$ on a 64^3 (red line) and 128^3 (blue line) mesh. Circles denote the DNS reference on the 256^3 mesh Johnsen *et al.* (2010).

1 Conclusions

1. The proposed TENO8-A scheme is 6th-order accurate and features sharp shock-capturing capability, low numerical dissipation and optimized dispersion property while maintaining good robustness. For gas dynamics involving strong discontinuities and broadband physical fluctuations, TENO8-A performs much better than WENO-CU6 in resolving small-scale flow structures without numerical oscillations and strong overshoots.
2. For the incompressible infinite Reynolds number TGV turbulence, TENO8-A can reproduce the self-similar Kolmogorov scaling with ROE-type flux for almost the entire resolved wavenumber range while with Rusanov flux for more than $2/3$ of the cut-off wavenumbers. For the viscous finite Reynolds number simulation, without parameter turning, the performance of TENO8-A is even better than the state-of-the-art ILES ALDM model in predicting the kinetic energy evolution.
3. For the compressible isotropic turbulence decay, TENO8-A faithfully computes the vorticity, entropy and acoustic models. The performance of TENO8-A in predicting the density, velocity and temperature fluctuations is at least comparable to the state-of-the-art localized artificial diffusivity scheme while for the dilatation computing it is remarkably better.

REFERENCES

Arshed, Ghulam M & Hoffmann, Klaus A 2013 Minimizing errors from linear and nonlinear weights of weno scheme for broadband applications with shock waves. *Journal of Computational Physics* **246**, 58–77.

Brachet, Marc E, Meiron, Daniel I, Orszag, Steven A, Nickel, BG,

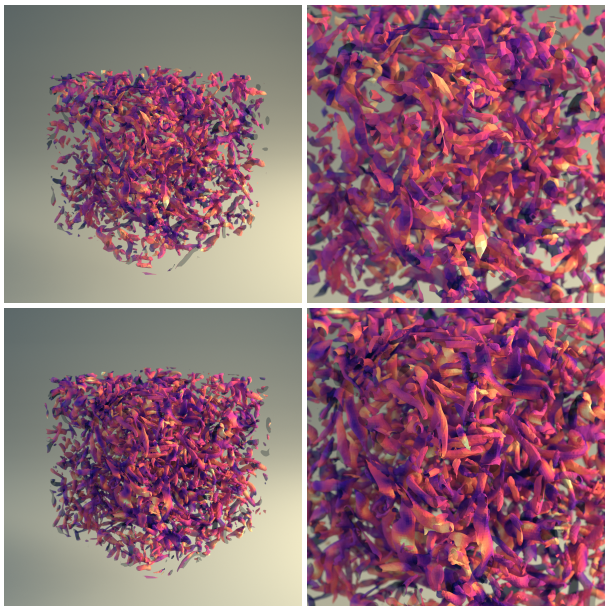

Figure 8. Compressible isotropic turbulence decay: the overall view (left) and zoom-in view (right) of iso-surface $Q = 5$ colored by the dilatation. Resolution of 64^3 (top) and 128^3 (bottom).

Morf, Rudolf H & Frisch, Uriel 1983*a* Small-scale structure of the taylor–green vortex. *Journal of Fluid Mechanics* **130**, 411–452.

Brachet, Marc E., Meiron, Daniel I., Orszag, Steven A., Nickel, B. G., Morf, Rudolf H. & Frisch, Uriel 1983*b* Small-scale structure of the taylor-green vortex. *Journal of Fluid Mechanics* **130**, 411–452.

Castro, Marcos, Costa, Bruno & Don, Wai Sun 2011 High order weighted essentially non-oscillatory weno-z schemes for hyperbolic conservation laws. *J. Comput. Phys.* **230**, 1766–1792.

Egerer, Christian P, Schmidt, Steffen J, Hickel, Stefan & Adams, Nikolaus A 2016 Efficient implicit les method for the simulation of turbulent cavitating flows. *Journal of Computational Physics* .

Fu, Lin, Hu, Xiangyu Y & Adams, Nikolaus A 2016 A family of high-order targeted eno schemes for compressible-fluid simulations. *Journal of Computational Physics* **305**, 333–359.

Gerolymos, GA, Sénéchal, D & Vallet, I 2009 Very-high-order weno schemes. *Journal of Computational Physics* **228** (23), 8481–8524.

Gottlieb, Sigal, Shu, Chi-Wang & Tadmor, Eitan 2001 Strong stability-preserving high-order time discretization methods. *SIAM review* **43** (1), 89–112.

Hickel, Stefan, Adams, Nikolaus A. & Domaradzki, J. Andrzej 2006 An adaptive local deconvolution method for implicit les. *J. Comput. Phys.* **213** (1), 413–436.

Johnsen, Eric, Larsson, Johan, Bhagatwala, Ankit V, Cabot, William H, Moin, Parviz, Olson, Britton J, Rawat, Pradeep S, Shankar, Santhosh K, Sjögreen, Björn, Yee, HC *et al.* 2010 Assessment of high-resolution methods for numerical simulations of compressible turbulence with shock waves. *Journal of Computational Physics* **229** (4), 1213–1237.

Kawai, Soshi, Shankar, Santhosh K & Lele, Sanjiva K 2010 Assessment of localized artificial diffusivity scheme for large-eddy simulation of compressible turbulent flows. *Journal of Computational Physics* **229** (5), 1739–1762.

Kotov, DV, Yee, HC, Wray, AA, Sjögreen, B & Kritsuk, AG 2016 Numerical dissipation control in high order shock-capturing schemes for les of low speed flows. *Journal of Computational Physics* **307**, 189–202.

Lesieur, Marcel 2012 *Turbulence in fluids*, , vol. 40. Springer Science & Business Media.

Rusanov, V V 1961 Calculation of interaction of non-steady shock waves with obstacles. *USSR J. Comp. Math. Phys.* pp. 267 – 279.

Schranner, Felix S, Hu, Xiangyu Y & Adams, Nikolaus A 2013 A physically consistent weakly compressible high-resolution approach to underresolved simulations of incompressible flows. *Computers & Fluids* **86**, 109–124.

Shi, J, Zhang, Y T & Shu, C W 2003 Resolution of high order weno schemes for complicated flow structures. *J. Comput. Phys.* **186**, 690–696.

Woodward, P 1984 The numerical simulation of two-dimensional fluid flow with strong shocks. *J. Comput. Phys.* **54**, 115–173.